Low-power-pumped high-efficiency frequency doubling at 397.5 nm in a ring cavity

Yan Li (李 岩)[1,2#], Zhiyuan Zhou (周志远)[1,2#], Dongsheng Ding (丁冬生)[1,2], and Baosen Shi (史保森)[1,2*]

[1]*Key Laboratory of Quantum Information, University of Science and Technology of China, Hefei 230026, China*

[2]*Synergetic Innovation Center of Quantum Information & Quantum Physics, University of Science and Technology of China, Hefei 230026, China*

[*]*Corresponding author: drshi@ustc.edu.cn*

[#]*These two authors contributed equally to this work.*

Received June 6, 2014; accepted July 16, 2014; posted online October 29, 2014

We report low pump power high-efficiency frequency doubling of a fundamental laser beam at 795 nm, corresponding to the rubidium D1 line, to generate UV light at 397.5 nm using a periodically poled $KTiOPO_4$ (PPKTP) crystal in a ring cavity. We obtain maximum stable output power of 49 mW for mode-matching pump power of 110 mW, corresponding to 45% raw efficiency (56% net efficiency when considering the output coupling mirror's 80% transmission). This is the highest efficiency obtained at this wavelength in PPKTP with such low pump power. We obtain 80% beam coupling efficiency to single-mode fiber, demonstrating high beam quality.

OCIS codes: 190.2620, 140.4780.

doi: 10.3788/COL201412.111901.

In laser optics, frequency doubling (FD) is a fundamental technique used to extend the frequency range of the existing lasers in a laboratory. FD is commonly used to generate high-power blue laser beams from near-infrared lasers that would be difficult to achieve by other methods. Blue laser sources are very important in several applications, including optical spectroscopy[1,2], nonlinear optics[3], and quantum information[4–6]. In quantum information processing, one of the fundamental tasks is the transfer and manipulation of the quantum resources between light and matter[7,8] (whether solid-state materials or atomic ensembles). The most commonly used quantum resources are the squeezed vacuum[4] and single-photon sources[5,6,9,10]. To couple a single photon to our cold rubidium ensembles, which have been trapped using a magneto-optical trap[11], a narrow bandwidth photon source is required. To operate an optical parametric oscillator (OPO) far below its threshold, we can obtain a single-photon source that meets the above requirements. To pump the OPO, we require a blue laser with exact FD of the rubidium D1 line (795 nm). Here we present the first part of this project. The FD technique has been in development for decades. In the early stages, FD was conducted using birefringent phase-matching crystals. In 1991, 650 mW of 430 nm light was generated using $KNbO_3$ in a ring cavity, and the conversion efficiency reached 48%[12]. For efficient conversion of light with birefringent phase-matching crystals, high pump power is needed, and the power circulating inside the cavity is very high, meaning that the crystal will suffer from serious thermal effects. The later emergence of quasi-phase-matching (QPM) crystals has made it very easy to generate FD with low pump powers, because QPM has the benefits of a highly effective nonlinear coefficient and no walk-off effect. Using a periodically poled $KTiOPO_4$ (PPKTP) crystal in a ring cavity, 330 mW blue light at 426 nm was obtained with a conversion efficiency of 55% in 2007[13]. Recently, 680 mW of blue light was produced at 486 nm using a Brewster cut PPKTP crystal in a ring cavity[14]. In 2013, 158 mW of 426 nm light was obtained by pumping a monolithic PPKTP standing wave cavity, and the conversion efficiency of this scheme was 45%[15]. To date, the highest FD efficiency when using PPKTP was reported in Ref. [16], which realized a near-unity efficiency by FD from 1550 to 775 nm in a semi-monolithic standing wave cavity. The conversion efficiency of FD in PPKTP is strongly dependent on the material absorptions of both the fundamental light and the second harmonic (SH) light. A shorter wavelength means higher absorption, and the corresponding FD efficiency is lower.

The aim of this work is to produce a blue laser to pump an OPO operating far below threshold. For such an OPO, the typical pump power is approximately 10 mW or lower. We have achieved a maximum power of 49 mW with a relatively low pump power of 110 mW. This is the highest efficiency obtained at this wavelength when using a PPKTP crystal to the best of our knowledge. A coupling efficiency of 80% when coupling the SH beam to a single-mode fiber indicates the high beam quality of the SH beam. Because the pump power is comparatively low, the thermal effect is not very significant, meaning that the laser can operate stably for hours.

The properties of the PPKTP crystal are described and investigated first, and then the theoretical background of FD in a ring cavity and the cavity design are presented. After some theoretical description, we introduce our

 © 2014 Chinese Optics Letters

experiment, and some basic laser parameters are measured and discussed. Finally, we draw our conclusions.

The type-I PPKTP crystal (Raicol Crystals) has dimensions of 1 × 2 × 10 (mm); the crystal was periodically poled with periodicity of 3.15 μm to obtain QPM for SH generation (SHG) from 795 to 397.5 nm. Both crystal end faces have anti-reflective coatings at the wavelengths of 397.5 and 795 nm. The crystal is x-cut for pump beam propagation along the x-axis of the crystal. Before the crystal can be inserted into the cavity, we need to determine the phase-matching temperature of the crystal. The phase-matching temperature is determined by performing a single-pass experiment. Pump light of 200 mW at 795 nm from a Ti:sapphire laser (MBR 110, Coherent) is focused into the center of the crystal, with a spot size of approximately 50 μm, and after filtering the pump light using a dichromatic mirror, we measure the SH power as a function of the crystal temperature. The crystal temperature is controlled by a semiconductor Peltier device with stability of ±2 mK. The results are shown in Fig. 1. The phase-matching temperature is 64.3 °C, and the temperature bandwidth is 1 °C. We also measured the temperature wavelength tuning coefficient to be 0.06 nm °C^{-1}. The nonlinear conversion coefficient under the present focusing conditions is 0.006 W^{-1}.

For single-pass SHG, the conversion efficiency is very low. By using a cavity, the fundamental power can be enhanced many times, depending on the transmittance of the input coupler and the internal cavity losses. The enhancement factor is determined by[17]

$$\kappa = \frac{P_C}{P_1} = \frac{T}{\left[1-\sqrt{(1-T)(1-L)(1-\Gamma P_c)}\right]^2}, \quad (1)$$

where P_C is the circulating power build-up inside the cavity for input power P_1, T represents the input mirror's transmittance, and L is the round-trip linear loss factor (without T), the linear losses include the transmission of fundamental light in other mirrors due to imperfect coating, the linear absorption of the fundamental light inside the crystal, the reflection at the ending faces of the crystal because of imperfect anti-reflected coating, and the diffraction loss. Γ includes all nonlinear losses, and contains two terms: $\Gamma = E_{NL} + \Gamma_{abs}$, where E_{NL} is the SHG coefficient that is equal to the single-pass configuration, where $P_{SH} = E_{NL}P_c^2$; the proportion of the SH power absorbed inside the crystal is determined using $P_{abs} = \Gamma_{abs}P_c^2$.

For a particular pump power P_1, linear loss L, and SHG coefficient E_{NL}, there is an optimum input transmission factor T that maximizes the round-trip power P_c, and thus also maximizes the SH power P_2. The optimum T is $T_{opt} = L/2 + \sqrt{(L/2)^2 + \Gamma P_1}$.

Figure 2 shows a schematic representation of our experimental setup. The pump laser is a Ti:sapphire laser tuned to a wavelength of 795 nm. Part of the laser beam is coupled to a single-mode fiber to produce a better spatial mode to pump the SHG cavity. To ensure the stability of the pump laser, a Faraday isolator is placed before the fiber coupler to prevent backscattering. The pump polarization is controlled by two wave plates that are placed after the fiber output port. The beam then enters an electro-optical modulator (EOM) to create sidebands to lock the cavity to the TEM_{00} mode using the Pound–Drever–Hall method[18]. After modulation by the EOM, the pump light is mode matched to the cavity by a focusing system consisting of two lenses, L2 and L3. The reflected light from the input mirror M1 is detected by a fast detector D1, and the signal from D1 is mixed with the RF modulation signal from the EOM by a common signal generator. The mixed signal passes through a low-pass filter, and an error signal is generated. The error signal is then processed using a home-made servo control and a high-voltage amplifier to control the piezoelectric transducer that is attached to mirror M2. The detector D2 is used to monitor the status of the cavity. The generated SH beam is filtered using a dichromatic mirror.

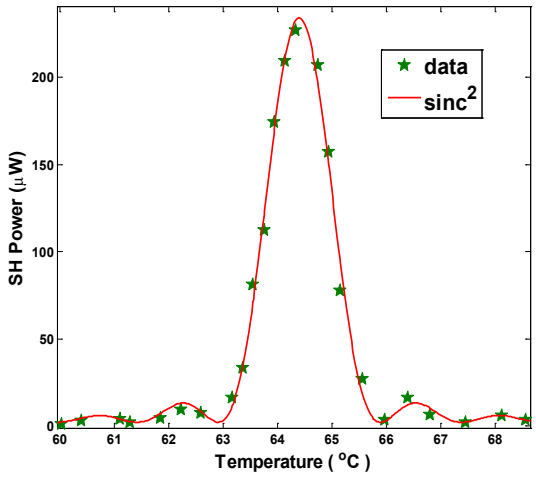

Fig. 1. Temperature tuning curve in the single-pass configuration. Green stars denote the experimental data, and the red curve is fitted using a sinc^2 function.

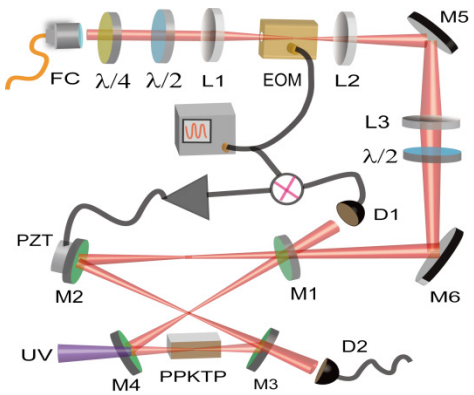

Fig. 2. Experimental setup for SHG of 795 nm light beam at 397.5 nm.

The ring cavity is formed by four mirrors, where the input coupling mirror M1 has a transmittance of 5% at 795 nm, and mirrors M2–M4 have highly reflective coatings at 795 nm ($R > 99.9\%$). The output mirror M4 alone has a transmittance of 80% at 397.5 nm (it does not have a high-transmission coating at 397.5 nm). Mirrors M3 and M4 are concave mirrors with 80 mm curvatures. The geometry of the cavity was designed using the ABCD matrix method; the cavity is operated in the region where $|A + D| \approx 0$, and the cavity is highly stable in this region. The calculated beam waist at the center of the crystal is 33 μm.

The reflected spectrum generated by scanning the cavity is detected by D1 and recorded using an oscilloscope, as shown in Fig. 3. The reflected spectrum reflects the status of the cavity, and we find that the small peaks that arise from the high-order cavity modes are inhibited to very low levels in our cavity; this ensures the long-term stable locking of the cavity. We also determined the mode-matching coefficient of the pump beam to be 80% from the reflected spectrum.

Then, we measured the SH power as a function of the pump power. The results are shown in Fig. 4. We obtained a maximum stable operating power of 49 mW for the SH beam with a mode-matched pump power of 110 mW, which corresponds to a 45% conversion efficiency. The net conversion efficiency is 56% when we take the 80% transmittance of the output coupler into account. The measured circulation power at pump power of 110 mW is 2.64 W. The SH wavelength is at the edge of the transparency window of the KTP crystal, and high UV absorption limits any further increase in the conversion efficiency. The absorption at 397.5 nm is approximately 0.20 cm^{-1}[19]. The red curve in Fig. 4 shows the results of a simulation based on the parameters of the experiment and using Eq. (1). In the simulation, the linear loss $L = 1.5\%$ and the nonlinear conversion coefficient $E_{NL} = 0.01\ W^{-1}$. In the low pump power region, the experimental data and the simulation results fit very well, but the experimental data deviate from the simulation results in the high pump power region. The differences between the two regions stem from the thermal effects of the crystal. The optimum phase-matching temperature will change when the circulation power increases. The increasing absorption of the SH light and the pump beam will induce a thermal lens effect, which makes the cavity unstable at high pump powers. The beam quality is quantified by coupling of the SH beam to a single-mode fiber; 80% coupling efficiency was achieved, which indicated the high quality of the beam's transverse spatial mode. The cavity can be locked at resonance for several hours.

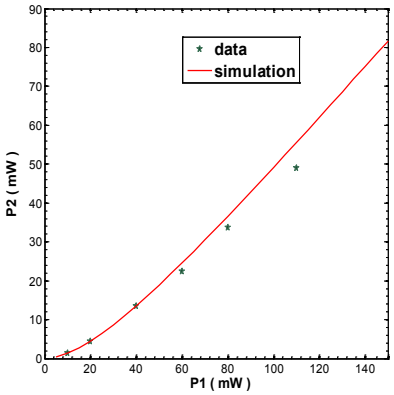

Fig. 4. SH power P_2 as a function of the fundamental power P_1. The stars represent the experimental data and the curve shows the results of a simulation using the experimental parameters.

The temperature tuning behavior of our cavity was also measured. Figure 5 shows the output SH power as a function of the crystal temperature with a fixed pump power of 60 mW. We read from the data that the optimum phase-matching temperature (63.4 °C) is approximately 1 °C lower than in the single-pass situation. This shows the direct impact of the thermal

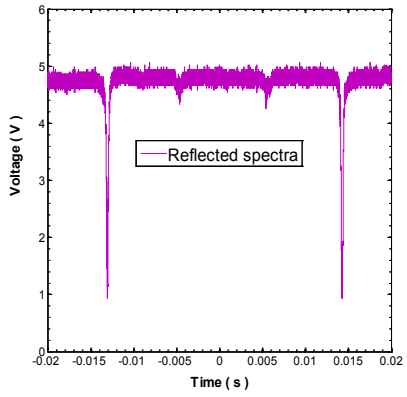

Fig. 3. Reflected spectrum of the cavity recorded using an oscilloscope by scanning the cavity.

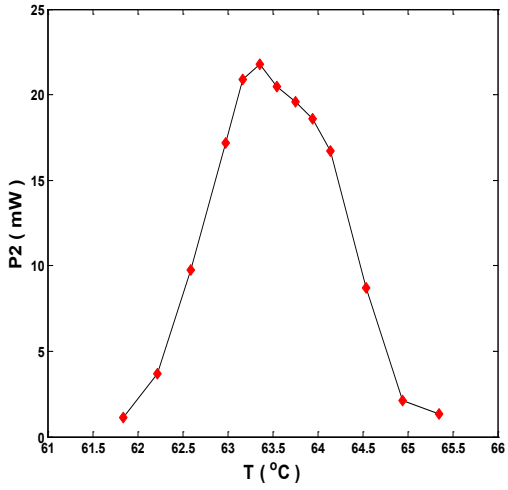

Fig. 5. Output SH power P_2 as a function of the crystal temperature.

effect, where the optimum phase-matching temperature decreases with increasing power circulating in the cavity.

In conclusion, we realize a high-efficiency UV laser at 397.5 nm based on cavity-enhanced SHG with low pump power. The high beam quality and long-term stability of the laser make it suitable for pumping of an OPO operating far below threshold. A total of 49 mW of UV light can be generated for a pump power of 110 mW. This relatively low pump power is a significant advantage for our setup. Some commercial SHG lasers are available that use angle phase-matching crystals to achieve widely tunable wavelengths. While these lasers have sufficiently low nonlinear coefficients when compared with QPM crystals, high pump powers are required for efficient conversion, and a taped amplifier (TA) is often needed. This increases both the complexity and the cost of these SHG systems. In some atomic experiments, wide wavelength tunability is not required. Given that scenario, our results make it possible to overcome the aforementioned disadvantages of the commercial SHG lasers.

For example, we require a 397.5 nm laser to pump an OPO to generate a photon-pair source. We expect the generated photon pair to be capable of interfacing with cold rubidium ensembles. Therefore, the wavelength of the photon pair must be at the D1 line of the rubidium atom. A tunable range of only 7 GHz is required to cover the full transition spectrum of the D1 lines.

In addition, the pump can be replaced with an external cavity diode laser (ECDL) without the need for a TA. This laser can directly pump the SHG system to generate the UV light. Another advantage of using the ECDL is that we can also remove the EOM and modulate the LD current directly. This will make the system more compact and enhance its performance. Also, fast current feedback can improve the locking performance of the SHG cavity, which leads to greater SH power stability. These advantages demonstrate the possibility of applying our system in commercial SHG lasers, particularly in atomic-level applications.

This work was supported by the National Fundamental Research Program of China (No. 2011CBA00200), the National Natural Science Foundation of China (Nos. 11174271, 61275115, and 10874171), and the Innovation Fund of the Chinese Academy of Sciences.

References

1. E. S. Polzik, J. Carri, and H. J. Kimble, Phys. Rev. Lett. **68,** 3020 (1992).
2. K. H. Ko, K. H. Lee, H. Park, J. Han, Y. H. Cha, G. Lim, T. S. Kim, and D. Y. Jeong, Chin. Opt. Lett. **10,** S21903 (2012).
3. S. Zhang, L. Guo, M. Li, L. Zhang, X. Yan, W. Hou, X. Lin, and J. Li, Chin. Opt. Lett. **10,** 071401 (2012).
4. S. Suzuki, H. Yonezawa, F. Kannari, M. Sasaki, and A. Furusawa, Appl. Phys. Lett. **89,** 061116 (2006).
5. Z. Y. Ou and Y. J. Lu, Phys. Rev. Lett. **83,** 2556 (1999).
6. F. Y. Wang, B. S. Shi, and G. C. Guo, Opt. Lett. **33,** 2191 (2008).
7. J. Appel, E. Figueroa, D. Korystov, M. Lobino, and A. I. Lvovsky, Phys. Rev. Lett. **100,** 093602 (2008).
8. H. Zhang, X. M. Jin, J. Yang, H. N. Dai, S. J. Yang, T. M. Zhao, J. Rui, Y. He, X. Jiang, F. Yang, G. S. Pan, Z. S. Yuan, Y. J. Deng, Z. B. Chen, X. H. Bao, S. Chen, B. Zhao, and J.W. Pan, Nat. Photon. **5,** 628 (2011).
9. B. S. Shi, F. Y. Wang, C. Zhai, and G. C. Guo, Opt. Commun. **281,** 3390 (2008).
10. X. H. Bao, Y. Qian, J. Yang, H. Zhang, Z. B. Chen, T. Yang, and J. W. Pan, Phys. Rev. Lett. **101,** 190501 (2008).
11. Y. Liu, J. H. Wu, B. S. Shi, and G. C. Guo, Chin. Phys. Lett. **29,** 024205 (2012).
12. E. S. Polzik and H. J. Kimble, Opt. Lett. **16,** 1400 (1991).
13. F. Villa, A. Chiummo, E. Giacobino, and A. Bramati, J. Opt. Soc. Am. B **24,** 576 (2007).
14. K. Danekar, A. Khademian, and D. Shiner, Opt. Lett. **36,** 2940 (2011).
15. X. Deng, J. Zhang, Y. C. Zhang, G. Li, and T. C. Zhang, Opt. Express **21,** 25907 (2013).
16 S. Ast, R. M. Nia, A. Schönbeck, N. Lastzka, J. Steinlechner, T. Eberle, M. Mehmet, S. Steinlechner, and R. Schnabel, Opt. Lett. **36,** 3467 (2011).
17. A. Ashkin, G. D. Boyd, and J. M. Dziendzic, IEEE J. Quant. Electron. **2,** 109 (1966).
18 R. W. P. Drever, J. L. Hall, F. V. Kowalski, J. Hough, G. M. Ford, A. J. Munley, and H. Ward, Appl. Phys. B **31,** 97 (1983).
19. F. Y. Wang, B. S. Shi, Q. F. Chen, C. Zhai, and G. C. Guo, Opt. Commun. **281,** 4114 (2008).